

# Observation of quantum oscillations between a Josephson phase qubit and a microscopic resonator using fast readout

K. B. Cooper,<sup>1</sup> Matthias Steffen,<sup>1,2</sup> R. McDermott,<sup>1</sup> R. W. Simmonds,<sup>1</sup>  
Seongshik Oh,<sup>1</sup> D. A. Hite,<sup>1</sup> D. P. Pappas,<sup>1</sup> and John M. Martinis<sup>1,\*</sup>

<sup>1</sup>National Institute of Standards and Technology, 325 Broadway, Boulder, CO 80305

<sup>2</sup>Center for Bits and Atoms - MIT, Cambridge, MA 02139

(Dated: November 18, 2018)

We have detected coherent quantum oscillations between Josephson phase qubits and microscopic critical-current fluctuators by implementing a new state readout technique that is an order of magnitude faster than previous methods. The period of the oscillations is consistent with the spectroscopic splittings observed in the qubit's resonant frequency. The results point to a possible mechanism for decoherence and reduced measurement fidelity in superconducting qubits and demonstrate the means to measure two-qubit interactions in the time domain.

Superconducting circuits based on Josephson tunnel junctions have attracted renewed attention because of their potential use as quantum bits (qubits) in a quantum computer[1]. Rapid progress toward this goal has led to the observation of Rabi oscillations in charge, flux, phase, and hybrid charge/flux based Josephson qubits[2, 3, 4, 5]. Another milestone toward building a scalable quantum computer is the coherent coupling of two qubits. While coupled-qubit interactions have been inferred spectroscopically[6, 7] and a two-qubit quantum gate has been implemented[8], the direct detection of correlations of qubit states in the time domain remains to be demonstrated. One obstacle to observing two-qubit dynamics is that the single-shot state readout time must be much shorter than the qubit coherence time ( $\sim 10 - 100$  ns) and the timescale of the coupled-qubit interaction. Fast readout techniques are also needed for error correction algorithms[9].

Here we report a state measurement of the phase qubit that has high fidelity and a duration of only 2 – 4 ns. Using this new readout technique, we directly detect time-domain quantum oscillations between the qubit and the recently discovered spurious resonators associated with critical-current fluctuators in Josephson tunnel junctions[10]. These results explicitly illustrate the mechanism by which critical-current fluctuators decohere phase qubits. We also present a model that attributes a reduction in measurement fidelity to the spurious resonators, and we speculate that qubit-fluctuator coupling contributes to decoherence and loss of fidelity in the flux and charge/flux qubits as well. In addition to revealing these new aspects of qubit physics, the few-nanosecond measurement technique will be valuable for future experiments on coupled qubits.

The design and fabrication of the Josephson phase qubits used in this experiment have been described previously[2, 10], and Fig. 1a shows their principal circuitry. The qubit consists of a superconducting loop containing a single Josephson junction. The qubit is inductively coupled to a line carrying a flux bias current

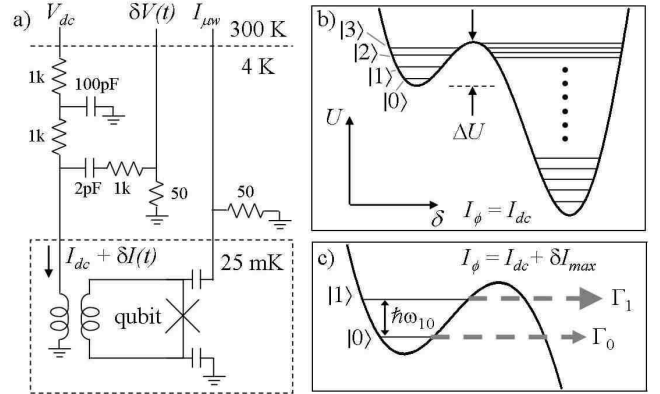


FIG. 1: (a) Schematic of the qubit circuitry. For the qubit used in Fig. 2, the Josephson critical-current and junction capacitance are  $I_0 \approx 10 \mu\text{A}$  and  $C \approx 2 \text{ pF}$ ; in Figs. 3 and 4, each of these values is about 5 times smaller. (b) Potential energy landscape and quantized energy levels for  $I_\phi = I_{dc}$  prior to the state measurement. (c) At the peak of  $\delta I(t)$ , the qubit well is much shallower and state  $|1\rangle$  rapidly tunnels to the right hand well.

$I_\phi = I_{dc} + \delta I(t)$ , where  $I_{dc}$  varies slowly and a short pulse  $\delta I(t)$  is used for the fast readout scheme. The microwave current  $I_{\mu w}$  induces Rabi oscillations, and it is capacitively coupled to the qubit after passing through low-temperature attenuators (not shown). The dashed box in Fig. 1a surrounds on-chip components kept near 25 mK. Figure 1b shows the potential energy landscape of the qubit's Josephson phase. The cubic confinement potential on the left contains several energy levels, with  $|0\rangle$  and  $|1\rangle$  representing the qubit states separated by an energy  $\hbar\omega_{10}$ . Both  $\hbar\omega_{10}$  and the depth of the left hand well,  $\Delta U$ , can be adjusted by varying the bias current  $I_\phi$ .

Rabi oscillations between states  $|0\rangle$  and  $|1\rangle$  can be observed by irradiating the qubit with microwaves at a frequency  $\omega/2\pi \approx \omega_{10}/2\pi \sim 5 - 10 \text{ GHz}$  and then measuring the qubit's probability of being in state  $|1\rangle$ . This probability was previously measured by applying microwaves at a frequency  $\omega_{31}$  for a duration of 80-100 ns, causing

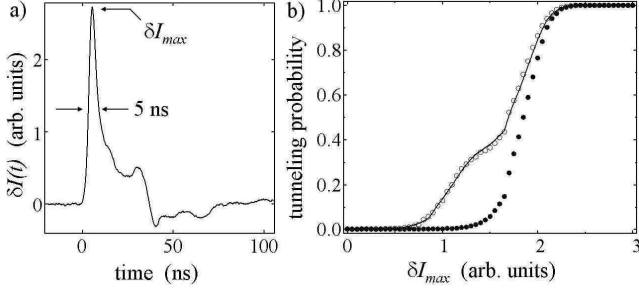


FIG. 2: (a) Room temperature measurement of the fast current pulse. (b) Tunneling probability versus  $\delta I_{max}$  with the qubit in state  $|0\rangle$  (solid circles) and in an equal mixture of states  $|1\rangle$  and  $|0\rangle$  (open circles). Fit to data is shown by the solid line. The plateau, being less than 0.5, corresponds to a maximum measurement fidelity of 0.63.

a  $1 \rightarrow 3$  transition when  $|1\rangle$  is occupied. Once in state  $|3\rangle$ , the Josephson phase rapidly tunnels into the right hand well, and subsequent measurement of the qubit's flux state with an adjacent dc SQUID (not shown in Fig. 1a) reveals whether the tunneling occurred. The measurement time of this method cannot be made significantly shorter than  $\sim 80$  ns because of the need to balance the strength of the  $1 \rightarrow 3$  transition against the tunneling rate of state  $|3\rangle$ .

We achieve a faster state measurement of the phase qubit by applying a short bias current pulse  $\delta I(t)$  that adiabatically reduces the well depth  $\Delta U/\hbar\omega_p$  so that the state  $|1\rangle$  lies very near the top of the well when the current pulse is at its maximum  $\delta I_{max}$  (see Fig. 1c). The value of  $\delta I_{max}$  is chosen so that the tunneling rate  $\Gamma_1$  of state  $|1\rangle$  at  $\delta I_{max}$  is high enough that  $|1\rangle$  will almost certainly tunnel over the duration of  $\delta I(t)$ . Also, because  $\Gamma_1$  is at least two orders of magnitude larger than the tunneling rate  $\Gamma_0$  of  $|0\rangle$ , a single current pulse yields a reliable measurement of the probability that  $|1\rangle$  is occupied. Calculations suggest that the ratio of tunneling rates for shallow wells is  $\alpha = \Gamma_1/\Gamma_0 \approx 150$ , and that the corresponding maximum measurement fidelity is  $\eta \approx \alpha^{-1/\alpha} - \alpha^{-1} \approx 0.96$ . Here  $\eta$  is defined as the difference of the tunneling probability when the qubit is in state  $|1\rangle$  versus state  $|0\rangle$ .

Room temperature measurements reveal that  $\delta I(t)$  has a width of about 5 ns, as shown in Fig. 2a. This is sufficiently slow to maintain adiabaticity with respect to the subnanosecond time scales associated with intrawell transitions. The actual measurement time will be somewhat shorter than the full width of  $\delta I(t)$  because the tunneling rate  $\Gamma_1$  is *exponentially* sensitive to the total bias current  $I_\phi$ . Therefore, the qubit will be far more likely to tunnel near the peak of  $\delta I(t)$  rather than its flanks, including the long trailing-edge of  $\delta I(t)$  arising from impedance mismatches in the current bias line. We estimate the effective measurement duration to be only 2–4 ns. This is

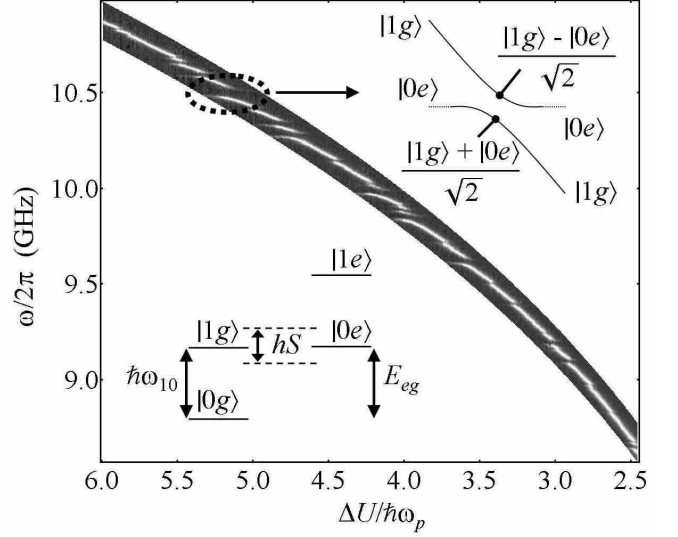


FIG. 3: Spectroscopy of  $\omega_{10}$  obtained using the current-pulse measurement method, as a function of well depth  $\Delta U/\hbar\omega_p$ . For each value of  $\Delta U/\hbar\omega_p$ , the grayscale intensity is the normalized tunneling probability, with an original peak height of 0.1 – 0.3. Inset: A given splitting in the spectroscopy of magnitude  $S$  comes from a critical-current fluctuator coupled to the qubit with strength  $hS/2$ . On resonance, the qubit-fluctuator eigenstates are linear combinations of the states  $|1g\rangle$  and  $|0e\rangle$ , where  $|g\rangle$  and  $|e\rangle$  are the two states of the fluctuator.

more than an order of magnitude shorter than the previously used microwave measurement technique as well as the readout methods used in most other superconducting qubits[11].

The data in Fig. 2b demonstrate the effectiveness of the fast measurement scheme. The solid circles correspond to the tunneling probability of the qubit as a function of the pulse height  $\delta I_{max}$  when no radiation at  $\omega_{10}$  is applied, i.e., when the qubit is in state  $|0\rangle$ . The data were obtained at an initial well depth of  $\Delta U = 4.5\hbar\omega_p$ , where  $\omega_p \approx \omega_{10}/0.9$  is the classical plasma frequency of the Josephson junction. The open circles in Fig. 2 are the measured tunneling probabilities as a function of  $\delta I_{max}$  after a microwave drive at  $\omega_{10}$  saturates the populations of  $|0\rangle$  and  $|1\rangle$  approximately equally. To produce a  $\approx 50/50$  mixture of  $|0\rangle$  and  $|1\rangle$ , microwaves were applied for 500 ns, much longer than the qubit's  $T_1$  time, and their power was high enough that the Rabi oscillation period of about 10 ns is shorter than  $T_1$ . The plateau in the tunneling probability data occurs around the values of  $\delta I_{max}$  where state  $|1\rangle$  has a high tunneling rate while state  $|0\rangle$  remains mostly confined in its potential well. For equal populations of  $|0\rangle$  and  $|1\rangle$ , the plateau should level out near 0.50 for the predicted measurement fidelity of  $\eta = 0.96$ . Instead, the measured tunneling probability plateaus around 0.35, suggesting a lower, but still good, fidelity. Indeed, fitting the tunneling data to a

simple model with a constant tunneling ratio  $\alpha$  yields a maximum fidelity of  $\eta = 0.63$  (solid line in Fig. 2). One possible reason for this lower fidelity will be discussed below.

The new state readout scheme is capable of measuring the spectroscopy of the  $0 \rightarrow 1$  transition for a broad range of well depths, as shown in Fig. 3. The data were obtained from a qubit with a slightly lower fidelity ( $\eta \approx 0.5$ ) than that of Fig. 2b, but both exhibit the same essential behavior. Similar spectroscopic data were shown in ref. [10], and the grayscale is proportional to the occupation probability of state  $|1\rangle$  after a long, low power microwave drive is applied. However, here the fast-pulse measurement method is used with  $\delta I_{max}$  adjusted to optimize the signal at each flux bias point. The new measurement method is capable of probing a much broader range of  $\Delta U/\hbar\omega_p$  than the old method, where the slow tunneling rate of  $|3\rangle$  limits the accessible well depths to less than about  $\Delta U/\hbar\omega_p = 3.5$ . Also, Fig. 3 shows a series of gaps in the  $\omega_{10}$  resonance signal, and these splittings likely reflect avoided level crossings arising from an interaction of the qubit with individual critical-current fluctuators at microwave frequencies[10]. Treating a single fluctuator as two-level quantum systems and labeling its ground and excited states as  $|g\rangle$  and  $|e\rangle$ , a coupling of strength  $hS/2$  will split the direct-product states  $|1g\rangle$  and  $|0e\rangle$  by  $hS$  when the qubit energy  $\hbar\omega_{10}$  is tuned to the fluctuator energy  $E_{eg}$  (see insets to Fig. 3). Splittings as large as  $S \approx 70$  MHz are visible in Fig. 3.

Simmonds *et al.* have already shown that the qubit's Rabi oscillations have reduced coherence when  $\omega_{10}$  is tuned near a splitting in the spectroscopy[10]. To better understand the spurious resonators' effect on the qubit, it is helpful to examine the *dynamics* of the qubit-fluctuator interaction directly, and the few-nanosecond readout method allows us to accomplish this. Figure 4a shows a section of the spectroscopy of Fig. 3 around  $\Delta U/\hbar\omega_p = 3.6$ , where a strong, well-isolated splitting occurs at  $\omega_{10}/2\pi = 9.62$  GHz with a magnitude of  $S \approx 44$  MHz. A smaller splitting of magnitude  $S \approx 24$  MHz is visible at a slightly shallower well depth. Figure 4b shows the time-domain response of the qubit to an 8 ns  $\pi$ -pulse for the qubit tuned to the center of (solid) and away from (dashed) the 44 MHz splitting in Fig. 4a. Following the  $\pi$ -pulse, the fast measurement probe is applied after a delay of  $\tau_D$  to measure how the occupation probability of  $|1\rangle$  changes with time. For a well depth  $\Delta U/\hbar\omega_p = 3.50$ , the dashed curve in Fig. 4b exhibits an exponential decay with a time constant that is roughly  $T_1 \approx 25$  ns[12]. In contrast, the solid curve in Fig. 4b shows that when the qubit is tuned to a large splitting, at  $\Delta U/\hbar\omega_p = 3.58$ , a striking beating in the tunneling probability is superimposed on the  $T_1$  decay curve. Although this beating represents a probability oscillation between  $|1\rangle$  and  $|0\rangle$ , it is *not* a Rabi oscillation because there is no microwave driving power at  $\omega_{10}$ . Instead, the beating period of 24

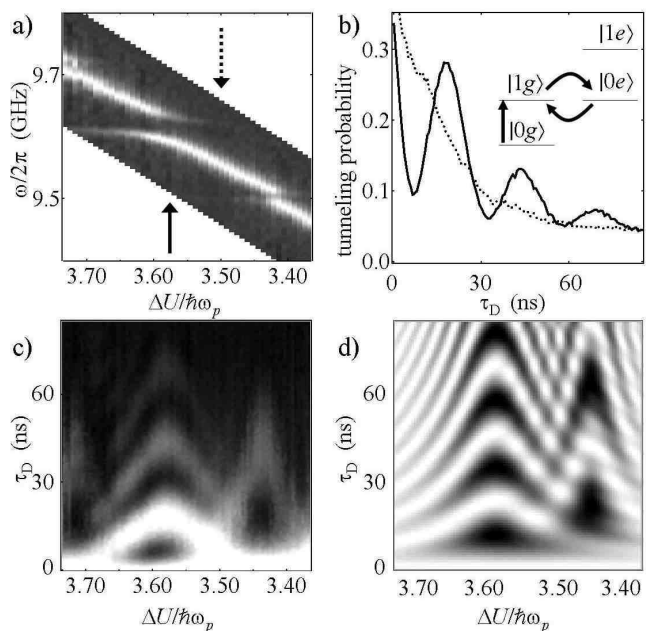


FIG. 4: (a) Detail of the qubit spectroscopy near  $\Delta U/\hbar\omega_p = 3.55$ , showing splittings of strengths  $S \approx 44$  MHz and 24 MHz. (b) Tunneling probability versus measurement delay time  $\tau_D$  after application of  $\pi$ -pulse. Solid (dashed) line is taken at a well depth of solid (dashed) arrow in (a), corresponding to a resonant (off-resonant) bias. Inset illustrates how the qubit probability amplitude first moves to state  $|1g\rangle$  and then oscillates between  $|1g\rangle$  and  $|0e\rangle$ . (c) and (d) Tunneling probability (gray scale) versus well depth and  $\tau_D$  for experimental data (c) and numerical simulation (d). The peak oscillation periods are observed to correspond to the spectroscopic splittings.

ns is very close to the inverse of the measured splitting size  $S^{-1} = 23$  ns, which is expected from the model of the qubit coupled to a critical-current fluctuator with a strength  $S/2$ . As shown in the inset to Fig. 4b, after the qubit is promoted to state  $|1g\rangle$  by the  $\pi$ -pulse, the qubit-fluctuator interaction will cause an oscillation between  $|1g\rangle$  and  $|0e\rangle$  at a frequency  $S$  as energy is transferred back and forth between the qubit and the fluctuator. This constitutes compelling evidence for coherent quantum oscillations between the mesoscopic qubit and a single microscopic fluctuator.

A further test of this model is to track the time-domain response of the qubit over a narrow range of bias currents around the fluctuator's resonant frequency. As the qubit bias is moved away from resonance, we expect the beating frequency to increase as the states  $|1g\rangle$  and  $|0e\rangle$  become nondegenerate. This expectation is confirmed in Fig. 4c, which shows that the longest beating periods line up well with the major and minor splittings visible in Fig. 4a. By numerically modeling the qubit-fluctuator interaction based on the location and sizes of the splittings in Fig. 4a, we obtain the results in Fig. 4d (where dissipation is ignored). The simulation matches the experimental

results remarkably well, except for the exponential signal decay in Fig. 4c, as expected. However, note that our simulations and experimental results do not rule out the possibility that the resonator might have other excited levels out of resonance with the qubit.

We emphasize that these results could not have been obtained using the previous microwave measurement method because the signals would be averaged out over the  $\sim 100$  ns readout time. Probability beatings on longer time scales coming from more weakly coupled resonators could not be resolved either because of the qubit's short  $T_1$  times. The same limitations will exist if attempts are made to directly couple two qubits. Therefore, the new fast measurement presented here and the demonstration of dynamical coupling between the qubit and a critical-current fluctuator suggest that we now have the tools to successfully measure the coupling between two Josephson phase qubits.

The data of Fig. 4 demonstrate explicitly how a single, large fluctuator will absorb the occupation probability of state  $|1\rangle$ . Interestingly, once the fluctuator absorbs the qubit energy after  $\sim 10$  ns, it does not immediately decay incoherently from  $|0e\rangle$  to  $|0g\rangle$ . In fact, the envelope of decay of the beating signal in Fig. 4b is about one to two times the  $T_1$  of the qubit away from a large resonator. This means that the decay time of a strong critical-current fluctuator is at least as long as the qubit's  $T_1$  time. We thus speculate that spin-echo techniques might be able to refocus some of the signal loss due to the spurious resonators[13]. Another feature of the qubit-fluctuator interaction still to be explored is the effect of many small fluctuators not resolved in the spectroscopy data. Analyses of the resonator distributions could reveal how strongly such an ensemble of coupled critical-current fluctuators would affect the qubit and whether this might be a factor in the short  $T_1$  observed.

Another consequence of the dynamic qubit-resonator interaction is reduced fidelity of the fast-pulse measurement itself. As  $\delta I(t)$  increases during a measurement,  $\omega_{10}$  decreases and the qubit moves in and out of resonance with many spurious resonators before any tunneling occurs. If the qubit is initialized in state  $|1\rangle$ , then each resonator absorbs a small amount of the  $|1\rangle$  probability amplitude during the measurement pulse, leaving the qubit with some amplitude in state  $|0\rangle$ . The probability of remaining in state  $|1\rangle$  after sweeping through a single fluctuator of strength  $\hbar S/2$  can be estimated from the Zener-Landau tunneling formula  $P(S) = \exp(-\pi^2 S^2 / \dot{f}_{10})$ , where  $\dot{f}_{10} = \dot{\omega}_{10}/2\pi$  is the rate of change of the qubit frequency during the sweep[14].

Accounting for the effect of a collection of  $N_{S_i}$  resonators of splitting size  $S_i$ , the total measurement fidelity becomes  $\eta \approx \prod_i P(S_i)^{N_{S_i}}$ . For the qubit used in Fig. 2, spectroscopic measurements indicate that the rms splitting size of the 45 visible splittings is  $S_{rms} \approx 30$  MHz. Assuming that  $\delta I(t)$  results in a frequency sweep rate of

$\dot{f}_{10} \approx 1$  GHz/ns, we find that the measurement fidelity would be reduced from  $\eta \approx 1$  to  $\eta \approx 0.7$ . The actual fidelity of the qubit of Fig. 3 is  $\eta = 0.63$ , and therefore the qubit-fluctuator interaction is likely a prominent source of fidelity loss in the fast-pulse measurement method. Somewhat counter-intuitively, the Landau-Zener model predicts that the fidelity should become *worse* as the measurement duration becomes *longer*. Preliminary experiments involving slower pulses of  $\delta I(t)$  are consistent with this prediction, but so far it has been difficult to separate the effect of fidelity loss from the signal loss due to short  $T_1$  times. Nonetheless, this effect may have consequences for other superconducting qubit systems because similar current pulse schemes for state measurement and manipulation have been employed in the flux and the charge/flux qubits[4, 5]. Both qubits also exhibit significantly reduced fidelities of  $\eta \sim 0.6$ . However, in the case of the charge qubit a probability plateau analogous to that of Fig. 2b is absent, and the fidelity is estimated indirectly from the amplitude of Rabi oscillations[15]. Whether these lowered fidelities can be also attributed to microscopic fluctuators remains to be investigated.

In conclusion, we have implemented a state measurement technique for the Josephson phase qubit that is an order of magnitude faster than the microwave measurement method. With a temporal resolution of less than 5 ns, the fast-pulse method reveals coherent quantum oscillations between the qubit and a microscopic resonator embedded within the qubit circuit. The dynamics of the qubit-resonator interaction illustrate one mechanism by which the coherence of a superconducting qubit is lost to its environment. The size and number of the resonators also suggest that they are relevant to fidelity loss in pulse measurements, and we predict that the fidelity should increase as the measurement duration decreases. These results underscore the importance of understanding the details of Josephson junction physics in order to explain the quantum behavior of superconducting qubits. They also prove that all the tools are available for a time-domain demonstration of the coupling of two superconducting phase qubits.

This work was supported in part by NSA under contract MOD709001.

---

\* Electronic address: martinis@boulder.nist.gov

- [1] M.A. Nielsen and I.L. Chuang, *Quantum Computation and Quantum Information* (Cambridge University Press, Cambridge, 2000).
- [2] J.M. Martinis *et al.*, Phys. Rev. Lett. **89**, 117901 (2002).
- [3] Y. Nakamura *et al.*, Nature **398**, 786 (1999).
- [4] I. Chiorescu *et al.*, Science **299**, 1869 (2003).
- [5] D. Vion *et al.*, Science **296**, 886 (2002).
- [6] A.J. Berkley *et al.* Science **300**, 1548 (2003).
- [7] Y.A. Pashkin *et al.* Nature **421**, 823 (2003).

- [8] T. Yamamoto *et al.*, Nature **425**, 941 (2003).
- [9] D.P. DiVincenzo, Fortschr. Phys. **48**, 771 (2000).
- [10] R.W. Simmonds *et al.*, cond-mat/0402470 (2004).
- [11] Very recently, fast (2-5 ns) state measurements were reported in flux qubits and in a dc-SQUID circuit. See P. Bertet *et al.*, cond-mat/0405024 (2004); J. Claudon *et al.*, cond-mat/0405430 (2004).
- [12] The expected  $T_1$  times are on the order of microseconds, and the cause of the fast energy relaxation is under investigation.
- [13] N. Linden *et al.*, Chem. Phys. Lett. **305**, 28 (1999).
- [14] C. Zener, Proc. Roy. Soc. London A **137**, 696 (1932).
- [15] D. Vion (private communication).